Characterization of Time Variation on 1.9 GHz Fixed Wireless Channels in Suburban Macrocell Environments

Anthony E.-L. Liou, *Student Member, IEEE,* Kyle N. Sivertsen, *Student Member, IEEE,* and David G. Michelson, *Senior Member, IEEE*

***Abstract*—We observed temporal fading on 1.9 GHz fixed wireless channels during short-term measurements at 107 different locations in a suburban macrocell environment characterized by flat terrain and heavy foliage in order to determine how the rate of fading varies with average wind speed and distance. For each location, we estimated: (1) the Ricean K-factor using a moment-based estimator and (2) an equivalent Doppler frequency which is related to the maximum Doppler frequency by a factor that depends upon the shape of the Doppler spectrum. We did so by fitting the measured level crossing rate (LCR) and average fade duration (AFD) distributions to expressions normally justified for mobile wireless links using a method recently proposed by Feick, Valenzuela and Ahumada (2007). As has been observed at other sites, the Ricean K-factor decreased with both average wind speed and distance. However, we found that the equivalent Doppler frequency was effectively uncorrelated with wind speed and noticeably increased with distance. Similar measurements at other sites will be required to determine the extent to which these trends are affected by foliage density and tower height.**

***Index Terms*—Doppler measurements, fading channels, fixed wireless system, macrocell, multipoint communications system.**

I. Introduction

A GROWING number of fixed wireless point-to-multipoint communication systems that are deployed in suburban environments operate in the frequency range from 800 MHz to 6 GHz. It has long been recognized that wind blowing through foliage is a major cause of deep fading on the links in such systems. Together, the depth and rate of fading have significant implications for: (1) the implementation and tuning of automatic gain control and automatic power control loops [1], and (2) schemes such as opportunistic scheduling that take advantage of fast time fluctuations in the radio channel to improve system performance by favoring users at a time when they have higher data rates [2]. If the signal fluctuations occur too slowly, the performance of the opportunistic scheduler will be impaired and mitigation strategies must be devised, *e.g.*, [3]. The tendency for the Ricean K-factor to decrease as wind speed and/or distance increases has been noted and models that relate K to the two parameters in various environments have been proposed [4]-[10]. However, with the exception of a few anecdotal results, relatively little has been done to characterize the manner in which average wind speed and the distance of the terminal from the base station affect the *rate* of fading [11].

The rate at which signal fading occurs may be characterized either by the Level Crossing Rate (LCR) and Average Fade Duration (AFD) at selected thresholds above and below the mean signal strength [12] (which depend on both the first- and second-order statistics of the fading signal) or by a Doppler power spectrum [13],[14] (which depends only upon the second-order statistics). Although the latter representation is particularly useful because it is a key input for algorithms used to simulate (or emulate) fading channels, *e.g.*, [15],[16], estimation of the Doppler power spectrum generally requires coherent time series data (amplitude and phase). Fading on fixed wireless links occurs so slowly, however, that lack of phase coherence between the local oscillators in the widely separated transmitter and receiver can severely distort the result. Although a method for estimating the Doppler spectrum from amplitude-only measurement data was proposed in [14], it is intended mainly for use on short-range line-of-sight paths where the Ricean K-factor is high, *e.g.*, $K > 10$, and is much less effective in suburban macrocell environments where K is often < 10.

In certain cases, it has been found that one can fit the measured LCR and/or AFD distributions seen on fixed wireless links to expressions that are normally justified only for mobile wireless links [12]. This allows one to express the time variation on the link in terms of just three parameters: the mean signal strength, the Ricean K-factor, and an equivalent Doppler frequency which is referred to as $f_{d,FW}$ in [12] and which we will simply refer to as f_d. Here, based upon short-term measurements collected at 107 different locations in a suburban macrocell environment characterized by flat terrain and heavy foliage, we present what we believe is the first effort to describe the manner in which both K and f_d on 1.9 GHz fixed wireless links vary with both distance and average wind speed across a typical suburban macrocell. We also show how changing the shape of the Doppler spectrum affects the relationship between the estimated parameter f_d and the corresponding maximum Doppler frequency $f_{d,max}$.

The remainder of this paper is organized as follows: In Section II, we consider the model and method for estimating f_d that was proposed in [12] in greater detail. In Section III, we describe the measurement setup that we used to collect our data. In Section IV, we describe how we reduced the data and present our results. In Section V, we summarize our contributions and their implications.

Manuscript received March 11, 2008; revised February 12, 2009; accepted April 27, 2009. The associate editor coordinating the review of this letter and approving it for publication was S. Ghassemzadeh.

The authors are with the Radio Science Laboratory, Department of Electrical and Computer Engineering, University of British Columbia, Vancouver, BC, Canada, V6T 1Z4 (e-mail: {eliou, ksiverts, davem}@ece.ubc.ca).

This work was supported in part by grants from Bell Canada, Britsh Columbia Hydro and Power Authority, Tantalus Systems and Western Economic Diversification Canada.

Digital Object Identifier 10.1109/TWC.2009.090211

II. The Model

The complex envelope of the time-varying path gain $g(t)$ of either a mobile or fixed wireless link can usually be modelled as

$$g(t) = V + v(t), \tag{1}$$

where V is a fixed component and $v(t)$ is a zero-mean complex Gaussian process. If the power envelope $r(t)$ is given by

$$r\left(t\right) = \left|g\left(t\right)\right|^2, \tag{2}$$

the first-order statistics of r will follow a Ricean distribution where

$$\begin{aligned} p(r) =& \frac{2r\left(K+1\right)}{\Omega} exp\left(-K - \frac{r^2\left(K+1\right)}{\Omega}\right) \\ & \cdot I_0\left(2r\sqrt{\frac{K\left(K+1\right)}{\Omega}}\right), \end{aligned} \tag{3}$$

Ω is the average envelope power and $I_0(\cdot)$ is the zero order modified Bessel function of the first kind. In such cases, the Ricean K-factor is given by

$$K = \left|V\right|^2 / \overline{\left|v\left(t\right)\right|^2} = \left|V\right|^2 / \sigma^2, \tag{4}$$

where σ^2 is the power in the time-varying component $v(t)$. Various methods for estimating K have been proposed. Here, we use the moment-based method described in [17] where

$$K = \frac{\left|V\right|^2}{\sigma^2} = \frac{\sqrt{G^2 - \sigma_G^2}}{G - \sqrt{G^2 - \sigma_G^2}}, \tag{5}$$

and σ_G is the rms fluctuation of the envelope $r(t)$ about the mean; it is given by the standard deviation of $\left|g\left(t\right)\right|^2$.

In cases where the base station is fixed, the terminal is in motion, and scattering is two-dimensional and isotropic, the Doppler spectrum of the time-varying component is given by Clarke's U-shaped spectrum and ranges from -$f_{d,max}$ to $f_{d,max}$. The frequency offset of the carrier that corresponds to the fixed component is determined by the direction of the propagation path relative to the velocity of the terminal. In such cases, the LCR and AFD are given by

$$\begin{aligned} \text{LCR} =& \sqrt{2\pi\left(K+1\right)} f_d \rho \exp\left(-K - \left(K+1\right)\rho^2\right) \\ & \cdot I_0\left(2\sqrt{K\left(K+1\right)\rho}\right) \end{aligned} \tag{6}$$

and

$$\text{AFD} = \frac{\left(1 - Q\left(\sqrt{2K}, \sqrt{2\left(K+1\right)\rho^2}\right)\right) \exp\left(K + \left(K+1\right)\rho^2\right)}{\sqrt{2\pi\left(K+1\right)} f_d \rho I_0\left(2\sqrt{K\left(K+1\right)\rho}\right)} \tag{7}$$

where T is the threshold voltage, $\rho = T/r_{rms}$ is the threshold normalized to the rms envelope, $Q(\cdot)$ is the Marcum-Q function and, in this case, f_d corresponds to $f_{d,max}$.

In cases where both the base station and the terminal are fixed, time variation is due entirely to the motion of scatterers in the environment and the corresponding Doppler spectrum generally exhibits a sharp peak at the carrier frequency and rapidly decays as the frequency offset increases, $e.g.$, [13]. In [12], it was shown that under certain conditions the expressions for LCR and AFD given in (6) and (7) do not depend on the shape of the Doppler spectrum. In particular, applying the value of K estimated using (5) to (6) and (7), and choosing an appropriate value for f_d will often provide a good approximation to the LCR and AFD characteristics observed on fixed wireless links. Further, it was reported that a good estimate of f_d can be obtained by considering only the Zero Crossing Rate, ZCR, which is defined as the value of LCR for $\rho = 1$, $i.e.$,

$$\begin{aligned} \text{ZCR} =& \sqrt{2\pi\left(K+1\right)} f_d \exp\left(-2K - 1\right) \\ & \cdot I_0\left(2\sqrt{K\left(K+1\right)}\right). \end{aligned} \tag{8}$$

While (8) can easily be solved for f_d, the result is virtually insensitive to the actual value of the K-factor for $K > 3$. In such cases,

$$f_d \approx 1.4 ZCR \tag{9}$$

is a convenient approximation.

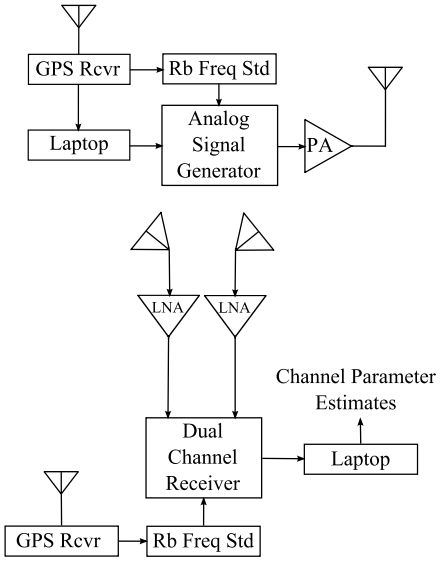

Fig. 1. Dual-channel sounder system set up.

III. Measurement Setup

A. CW Channel Sounder

Our CW channel sounder consists of a 1.9 GHz CW transmitter that we carried aboard our drive test vehicle and a dual-channel narrowband measurement receiver that we installed at our base station. A block diagram of the measurement setup is presented in Figure 1. We used a Marconi 2031 RF signal generator and an RF power amplifier to bring the transmitted power level up to 6 Watts, and a Bird digital RF power meter to measure the precise value. We used a 1.9 GHz vertically polarized omnidirectional sleeve dipole antenna with a gain of 2.2 dBi as our transmitting antenna. When used in non-line-of-sight configurations, fixed wireless antennas are

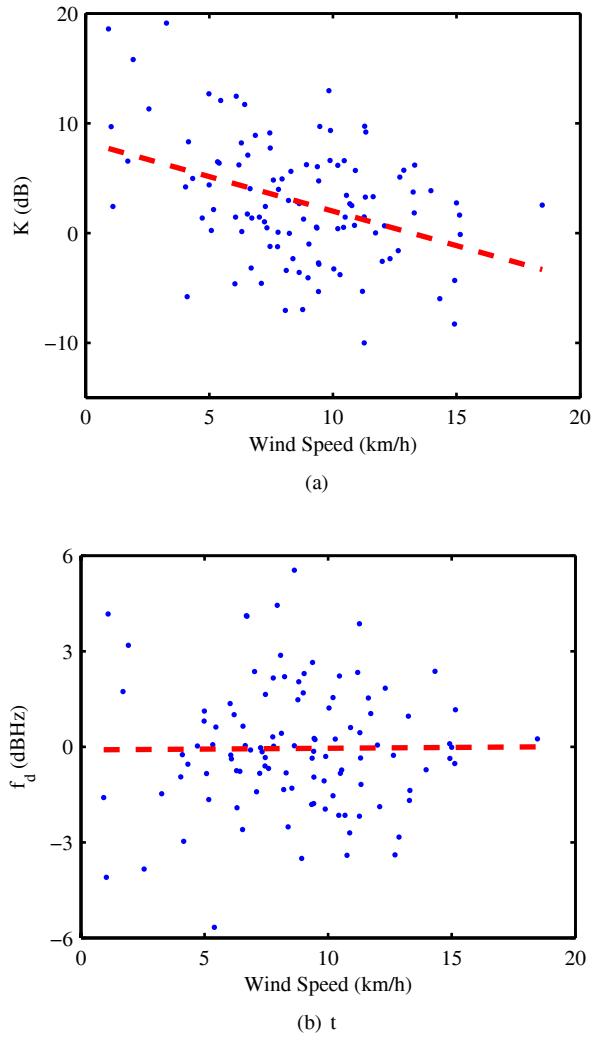

Fig. 2. (a) K-factor vs. distance and (b) equivalent Doppler frequency vs. average wind speed as observed at 107 locations across the test site.

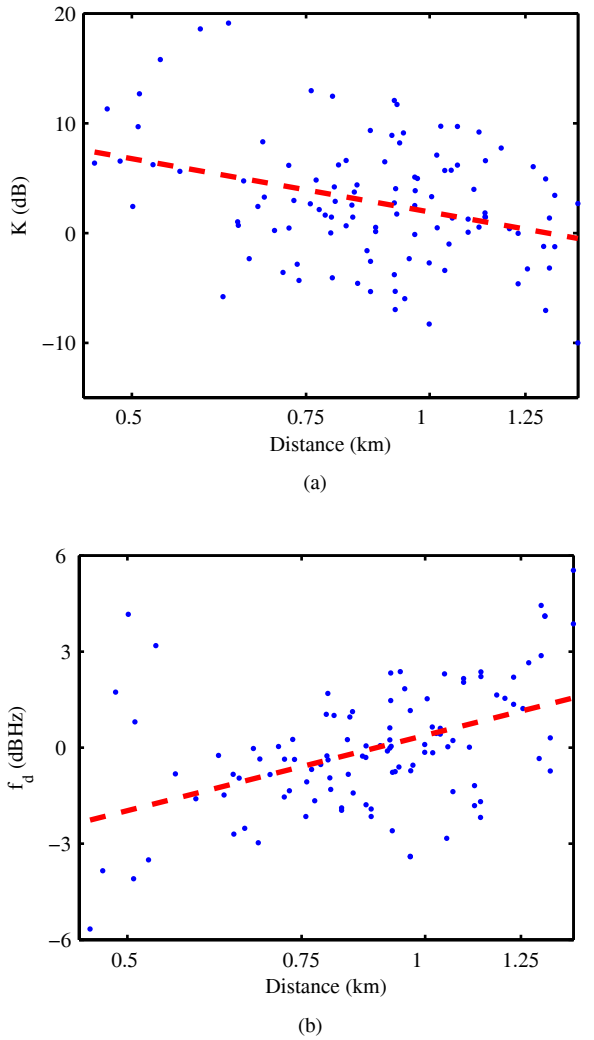

Fig. 3. (a) Ricean K-factor and (b) equivalent Doppler frequency, f_d, vs. distance as observed at 107 locations across the test site.

typically mounted at heights between 0.5 m (*e.g.*, for nomadic applications) and 4 m (*e.g.*, for permanent installations). As a compromise, we mounted the antenna on the center of the roof of our drive test vehicle at a height of 1.75 m.

We used a Cushcraft 1.9 GHz forward and back slant polarization diversity antenna with a gain of 7 dBi and beamwidth of 60 degrees as our receiving antenna. We mounted the antenna, mast and rotator atop a tower at a height of 25 m above ground level. When the drive test vehicle moved to a new location within the survey area, the receiving site operator rotated the antenna boresight towards it. We boosted the signals received on each branch by 25 dB using a pair of Mini-Circuit low noise amplifiers before we applied the signals to an HP 8753E vector network analyzer configured to operate as a dual-channel tuned receiver with an IF bandwidth of 30 Hz. We stabilized the frequencies of both the transmitter and receiver using Stanford Research Systems Rubidium frequency standards. Although outdoor temperatures were moderate during the measurement campaign, care was taken to protect the Rubidium frequency standard from sudden changes in ambient temperature, *e.g.*, as might be caused by sudden drafts of air.

Once per minute, we recorded the average wind speed estimated by a Davis Vantage Pro2 wireless weather station that we installed on a second tower located near the receiving site. Because previous work has shown that variations in average wind speed at tree top level or above are well correlated over mesoscale distances of several kilometers [18], we considered one wind measurement location near the base station to be adequate.

B. Calibration and Verification Protocol

Before we collected any field data, we verified the function and operation of our CW channel sounder using a Spirent SR5500 channel emulator configured in dual channel mode. We set the path gain and Ricean K-factor to a range of values. In each case, we confirmed that we were able to correctly estimate each parameter. We also selected alternative Doppler spectrum shapes, set the maximum Doppler frequency to a range of values and estimated the equivalent Doppler frequency using the method described in Section II. The results are presented in Section IV.

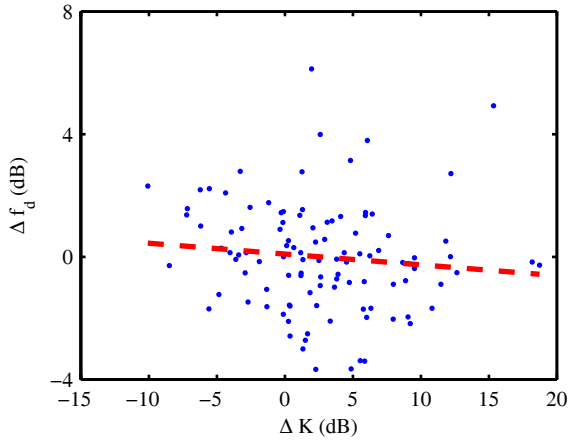

Fig. 4. The excess Ricean K-factor, ΔK, vs. the excess equivalent Doppler frequency, Δf_d, as observed at 107 locations across the test site.

C. Test Area

Our test area consisted of neighborhoods in and around the University of British Columbia and the surrounding University Endowment Lands. Within an annulus between 500 and 1500 m from our receiving site, we had access to both: (1) residential neighbourhoods with 8-12 m tall trees and heavy foliage throughout and (2) light urban areas with two- and four-storey buildings and somewhat less foliage. Almost all of the motion in the environment arose from wind-blown foliage; few, if any, cars, people or other moving scatterers were present in the vicinity when we collected measurement data. Most of the foliage in the area is coniferous but at least one-third is deciduous. All of the paths were obstructed; none of the remote had a line-of-sight to the base station. Because the duration of the measurement campaign was only six weeks, we had no opportunity to observe the effects of seasonal variations in the foliage, i.e., with trees in and out of leaf [19]. All of our data was collected with the trees in leaf.

D. Data Collection Protocol

Over a span of several weeks, the operator drove the drive test vehicle to each of the 107 survey locations that we had selected in advance and parked for approximately 20 minutes. Once the transmitter was running, the operator at the receiving site pointed the receiving antenna in the direction of the survey location, and then began recording time series measurements of the signal amplitudes (in dBm) received on the two diversity branches. The measured data were collected in the form of eight successive 120-second sweeps. Each of the eight sweeps contains 1601 samples collected at 0.075 second intervals or, equivalently, at a sample rate of 13.3 Hz. Collecting data at 107 locations in a variety of wind conditions took approximately six weeks.

IV. Results

Here we determine: (1) how changing the shape of the Doppler spectrum affects the relationship between the estimated parameter f_d and the corresponding maximum Doppler frequency $f_{d,max}$ and (2) the manner in which both K and f_d on 1.9 GHz fixed wireless links vary with both average wind speed and distance across a typical suburban macrocell.

When we claim or imply that a parameter or its residual follows a normal or lognormal distribution, we mean that it passed the Anderson-Darling test at the 5% significance level [20]. When we refer to linear regression analysis, we mean the least squares type. When we refer to a correlation coefficient, we mean Pearson's correlation coefficient.

A. Effect of Spectrum Shape on the Equivalent Doppler Frequency

If the remote terminal is in motion and scattering is two-dimensional and isotropic, the Doppler spectrum of the fading signal follows Clarke's model and f_d in (6) and (7) is given by

$$f_d = k f_{d,max}, \tag{10}$$

where $k = 1$. If the scattering is non-isotropic and/or the terminal is not in motion, the shape of the Doppler spectrum will be quite different. During the calibration and validation protocol described in Section III-B, we determined the value of k that applies to various Doppler spectrum shapes. We found that as the fraction of energy in the high frequency portion of the spectrum decreases, so does k. In particular, the 6-dB classic, flat and rounded spectra described in [21] yielded k = 0.91, 0.74 and 0.58, respectively. Further work is required to determine the corresponding relationship for spectra that are more typical of fixed wireless environments, $e.g.$, [13].

B. Dependence of the Ricean K-factor and Equivalent Doppler Frequency on Average Wind Speed

The average wind speed $\bar{\nu}_w$ observed at the base station during the short-term measurements followed a normal distribution with a mean value of 8.7 km/h and a standard deviation of 3.4 km/h. The manner in which the Ricean K-factor in dB decreased with the average wind speed across all measurement locations is presented in Figure 2(a). We attempted to fit both a line and an exponential decay to the data using least squares linear regression. The linear relationship is a better fit (as evidenced by a slightly higher correlation coefficient), so we opted to model the relationship between the Ricean K-factor and the average wind speed at this site by

$$K\,(\text{dB}) = -0.63\bar{\nu}_w + 8.27 + K_\sigma \tag{11}$$

where K_σ is a zero mean Gaussian random variable with standard deviation of 5.1 dB, $\bar{\nu}_w$ is in km/h and correlation coefficient $\rho = -0.38$.

The manner in which the equivalent Doppler frequency, f_d, in dBHz varied with the average wind speed is presented in Figure 2(b). As was observed in [11] at a handful of locations, the fading rate is essentially independent of wind speed. We applied linear regression analysis to determine that the relationship between the equivalent Doppler frequency and the average wind speed at this site. Because the two variables are essentially uncorrelated ($\rho < 0.009$), the relationship can be modeled by

$$f_d\,(\text{dBHz}) = -0.096 + f_\sigma \tag{12}$$

where f_σ is a zero mean Gaussian random variable with standard deviation of 1.97 dBHz.

C. Dependence of the Ricean K-factor and Equivalent Doppler Frequency on Distance

Our transmitter locations were situated between 500 and 1500 m away from the base station. The manner in which the Ricean K-factor in dB decreased with distance across all measurement locations is presented in Figure 3(a). We applied linear regression analysis to determine that the relationship between the Ricean K-factor and the distance at this site can be modeled by

$$K\,(\text{dB}) = -1.61\,(10\log_{10} d) + 1.92 + K_\sigma \tag{13}$$

where d is the distance in km, K_σ is a zero mean Gaussian random variable with standard deviation of 5.25 dB and the correlation coefficient $\rho = -0.33$.

The tendency for the equivalent Doppler frequency, f_d , in dBHz to rapidly increase with distance, as seen in Figure 3(b), has not been previously reported nor is it easily explained. We applied linear regression analysis to determine that the relationship between the equivalent Doppler frequency and distance at this site can be modeled by

$$f_d\,(\text{dBHz}) = 0.78\,(10\log_{10} d) + 0.38 + f_\sigma \tag{14}$$

where d is the distance in km, f_σ is a zero mean Gaussian random variable with standard deviation of 1.75 dBHz and the correlation coefficient $\rho = 0.46$.

Because both K_σ and f_σ are Gaussian random variables, they can be cast as a bivariate distribution for the purposes of simulation. Their joint distribution is depicted in Figure 4 where the excess Ricean K-factor ΔK and the excess equivalent Doppler frequency Δf_d are the deviations about the regression lines given in (13) and (14) that are captured by K_σ and f_σ. The parameters of the marginal distributions are as given above. With a correlation coefficient of 0.117, the two random variables are effectively uncorrelated.

V. Discussion

As has been observed at other macrocell sites, the Ricean K-factor decreased with both average wind speed and distance. Our observation that the equivalent Doppler frequency was effectively uncorrelated with wind speed corroborates anecdotal results reported in [11]. Our observation that equivalent Doppler frequency noticeably increased with distance was not anticipated by previous models or measurements. Similar measurements should be collected at other sites in order to determine the extent to which this trend: (1) is affected by foliage density and tower height or (2) might be predicted by suitably modified physical models of wind blown foliage, perhaps similar to those reported in [22] and [23].

References

[1] E. Armanious, D. D. Falconer, and H. Yanikomeroglu, "Adaptive modulation, adaptive coding, and power control for fixed cellular broadband wireless systems: some new insights," in *Proc. IEEE WCNC*, 2003, pp. 238-242.

[2] X. Liu, E. K. P. Chong, and N. B. Shroff, "Opportunistic transmission scheduling with resource-sharing constraints in wireless networks," *IEEE J. Select. Areas Commun.*, vol. 19, no. 10, pp. 2053-2064, Oct. 2001.

[3] P. Viswanath, D. N. C. Tse, and R. Laroia, "Opportunistic beamforming using dumb antennas," *IEEE Trans. Inform. Theory*, vol. 48, no. 6, pp. 1277-1294, June 2002.

[4] L. J. Greenstein, S. S. Ghassemzadeh, V. Erceg, and D. G. Michelson, "Ricean K-factors in narrowband fixed wireless channels: theory, experiments and statistical models," in *Proc. WPMC*, 1999.

[5] D. S. Baum *et al.*, "Measurements and characterization of broadband MIMO fixed wireless channels at 2.5 GHz," in *Proc. ICPWC*, 2000, pp. 203-206.

[6] V. Erceg *et al.*, "Channel models for fixed wireless applications," IEEE 802.16a-03/01, 27 June 2003.

[7] S. Perras and L. Bouchard, "Fading characteristics of RF signals due to foliage in frequency bands from 2 to 60 GHz," in *Proc. IEEE WPMC*, 2002.

[8] E. R. Pelet, J. E. Salt, and G. Wells, "Effect of wind on foliage obstructed line-of-sight channel at 2.5 GHz," *IEEE Trans. Broadcast.*, vol. 50, no. 3, pp. 224-232, 2004.

[9] D. Crosby, V. S. Abhayawardhana, I. J. Wassell, M. G. Brown, and M. P. Sellars, "Time variability of the foliated fixed wireless access channel at 3.5 GHz," in *Proc. IEEE VTC Spring 2005*, pp. 106-110.

[10] M. H. Hashim and S. Stavrou, "Wind influence on radio waves propagating through vegetation at 1.8 GHz," *IEEE Antennas Wireless Propag. Lett.,* vol. 4, pp. 143-146, 2005.

[11] M. H. Hashim, D. Mavrakis, and S. R. Saunders, "Measurement and analysis of temporal fading due to moving vegetation," in *Proc. IEEE ICAP*, 2003, pp. 650-653.

[12] R. Feick, R. A. Valenzuela, and L. Ahumada, "Experiment results on the level crossing rate and average fade duration for urban fixed wireless channels," *IEEE Trans. Commun.*, vol. 9, no. 1, pp. 175-179, Jan. 2007.

[13] S. Thoen, L. V. D. Perre, and M. Engels, "Modeling the channel time-variance for fixed wireless communications," *IEEE Commun. Lett.*, vol. 6, no. 8, pp. 331-333, Aug. 2002.

[14] A. Domazetovic, L. J. Greenstein, N. B. Mandayam, and I. Seskar, "Estimating the Doppler spectrum of a short-ranged fixed wireless channel," *IEEE Commun. Lett.*, vol. 7, no. 5, pp. 227-229, May 2003.

[15] K. E. Baddour and N. C. Beaulieu, "Accurate simulation of multiple cross-correlated Rician fading channels," *IEEE Trans. Commun.*, vol. 52, no. 11, pp. 1980-1987, Nov. 2004.

[16] B. Natarajan, C. R. Nassar, and V. Chandrasekhar, "Generation of correlated Rayleigh fading envelopes for spread spectrum applications," *IEEE Commun. Lett.*, vol. 4, no. 1, pp. 9-11, Jan. 2000.

[17] L. J. Greenstein, D. G. Michelson, and V. Erceg, "Moment-method estimation of the Ricean K-Factor," *IEEE Commun. Lett.*, vol. 3, no. 6, pp. 175-176, June 1999.

[18] S. R. Hanna and J. C. Chang, "Representativeness of wind measurements on a mesoscale grid with station separations of 312 m to 10 km," *Boundary-Layer Meteorol.*, vol. 60, pp. 309-324, 1992.

[19] ITU, "Attenuation in vegetation," Rec. ITU-R P.833-6, 2007.

[20] M. A. Stephens, "EDF statistics for goodness of fit and some comparisons," *J. Amer. Statistical Assoc.*, vol. 69, no. 347, pp. 730-737, Sept. 1974.

[21] "SR5500 Wireless Channel Emulator Operations Manual," Spirent Communications, Eatontown, NJ, 2006, pp. 3-16.

[22] D. A. J. Pearce, A. G. Burr, and T. C. Tozer, "Modelling and predicting the fading performance of fixed radio links through vegetation," in *Proc. IEEE NCAP*, 1999, pp. 263-266.

[23] P. Lédl, P. Pechač and M. Mazánek, "Time-series prediction of attenuation caused by trees for fixed wireless access systems operating in millimeter waveband," in *Proc. IEEE ICAP*, 2003, pp. 646-649.